engineering proceedings

Proceeding Paper

Smart Cushion System Based on Machine Learning and Pressure Sensing †

Mei-Chen Lee * and Ching-Fen Jiang

Graduate Degree Program of Smart Healthcare and Bioinformatics, I-Shou University, Kaohsiung 82445, Taiwan; cfjiang@isu.edu.tw

* Correspondence: l1046112005050@gmail.com

† Presented at the 2025 IEEE 5th International Conference on Electronic Communications, Internet of Things and Big Data, New Taipei, Taiwan, 25–27 April 2025.

Abstract

Prolonged poor sitting posture increases the risk of musculoskeletal disorders and chronic diseases. We developed a smart cushion system that integrated pressure sensing and machine learning for posture recognition. Nine FSR406 sensors were used to measure pressure distribution on the system. A calibration and normalization process improves data consistency, and a heatmap visualizes the result. Among the five machine learning models evaluated, the narrow neural network achieved the best performance, with a validation accuracy of 97.63% and a test accuracy of 91.73%. When body mass index (BMI) was included as an additional input feature, the test accuracy improved to 95.49%, indicating that BMI positively impacts recognition performance.

Keywords: sitting posture recognition; machine learning; pressure sensor

check for updates

Academic Editors: Teen-Hang Meen, Shu-Han Liao and Cheng-Fu Yang

Published: 8 September 2025

Citation: Lee, M.-C.; Jiang, C.-F. Smart Cushion System Based on Machine Learning and Pressure Sensing. *Eng. Proc.* **2025**, *108*, 39. https://doi.org/10.3390/engproc2025108039

Copyright: © 2025 by the authors. Licensee MDPI, Basel, Switzerland. This article is an open access article distributed under the terms and conditions of the Creative Commons Attribution (CC BY) license (https://creativecommons.org/licenses/by/4.0/).

1. Introduction

With the rapid advancement of digital technology, sedentary lifestyles have become increasingly common in both occupational and personal settings. On average, adults spend over half of their waking hours—approximately 8 to 10 h per day—in sedentary positions, including prolonged sitting during computer use, television viewing, or commuting [1]. The shift to remote work during the COVID-19 pandemic exacerbated this trend, with studies reporting increased sitting durations by up to 28% among workers working from home [2,3]. This sustained sedentary behavior is extensively linked to a wide range of adverse health outcomes, including obesity, cardiovascular disease, type 2 diabetes, metabolic syndrome, and certain cancers [4–6]. Furthermore, poor sitting posture, which often accompanies prolonged sitting, leads to musculoskeletal discomfort, spinal misalignment, and chronic pain conditions, particularly in the lower back, neck, and shoulders [7–9]. Notably, Tremblay et al. reported that extended sedentary time is independently associated with increased all-cause and cardiovascular mortality risks, particularly when daily sitting exceeds seven hours [4]. In addition, the combined impact of prolonged sitting and poor posture compromises long-term health and affects productivity and quality of life.

Sitting posture recognition technologies are applied to wearable and non-wearable systems. Wearable devices such as accelerometers and gyroscopes are commonly used for real-time motion tracking [10,11]. For instance, Wang et al. [10] applied a waist-mounted accelerometer for detecting seated postures using pattern recognition algorithms. While effective, such systems require users to wear multiple sensors, potentially affecting comfort

and long-term usability. Camera-based systems offer non-intrusive visual analysis [12–14]. Vishwakarma et al. [12] proposed a deep-learning-based model for posture classification using red-green-blue (RGB) images. Despite high accuracy, privacy concerns and sensitivity to lighting conditions limit their deployment in daily environments. Pressure-sensing solutions provide a balance between privacy, usability, and accuracy [15–18]. Huynh et al. [15] used an array of pressure sensors embedded in a seat cushion for continuous posture monitoring. While promising, these systems address issues such as sensor drift, individual variability, and long-term stability.

In this study, we developed a pressure-based smart cushion system using nine FSR406 sensors to recognize nine sitting postures: upright, leaning forward, backward, left, and right, as well as legs crossed at the knees and ankle over the knee on both the left and right sides. The system visualizes pressure distributions through heatmaps and integrates BMI-based grouping to improve classification accuracy.

2. Materials and Methods

2.1. Hardware Setup

The developed smart cushion system utilized nine force-sensitive resistors (FSR406) arranged in a 3 × 3 matrix to detect pressure variations across different seating regions (Figure 1). The FSR406 is an ultra-thin, resistive pressure sensor measuring 1.75 × 1.5 inches (approximately 45 × 38 mm). Its resistance decreases with increasing force, allowing for analog detection of pressure changes. The sensor is capable of detecting force in the range of 100 g to 10 kg, making it appropriate for monitoring typical seated pressure levels. The analog signals from the sensors were directly read by the analog input pins of an ESP32 NodeMCU-32S microcontroller board. ESP32 is a low-power, dual-core microcontroller unit (MCU) with integrated Wi-Fi and Bluetooth modules and features 12-bit analog-to-digital converter (ADC) resolution for accurate analog data acquisition. The collected voltage signals were transmitted to a computer and saved in CSV format for further processing.

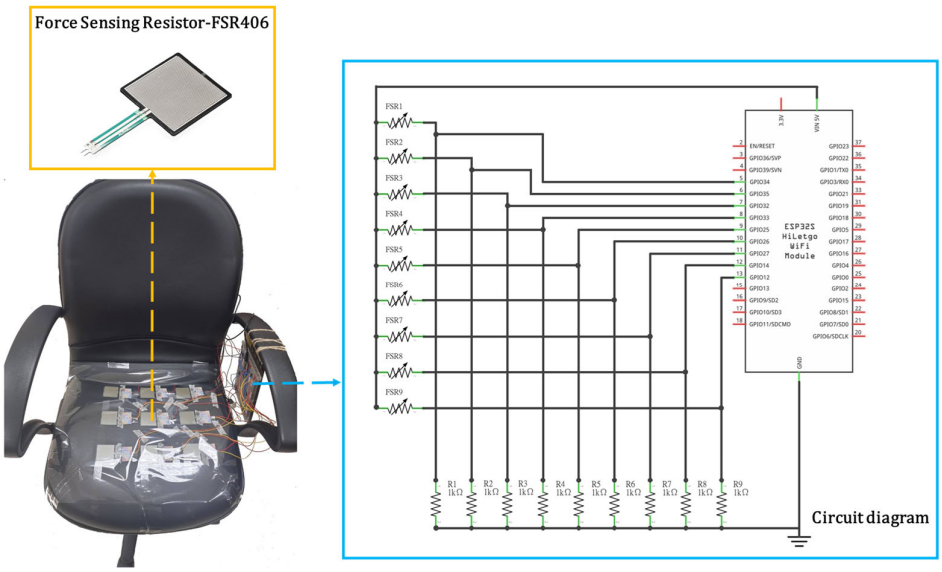


Figure 1. Hardware layout of the smart cushion system, including sensor placement and Circuit diagram.

2.2. Sensor Signal Calibration and Preprocessing

Due to the material characteristics of the FSR406 sensor, the measured voltage increases gradually over time even under a constant applied force. This phenomenon, known as creep [19], introduces errors during short-term measurements and reduces the reliability of

posture classification. To compensate for this, an exponential creep correction model was applied to the raw voltage data. The correction model is defined as Equation (1):

$$y(t) = y_0 + A\left(1 - e^{-kt}\right) \quad (1)$$

where $y(t)$ represents the time-dependent output voltage of the pressure sensor, reflecting both immediate and creep-induced deformation, the parameter y_0 denotes the initial output level of the pressure sensor at the moment loading begins, which reflects both immediate deformation and any baseline offset in the system, A indicates the total creep amplitude, representing the long-term deformation that occurs under sustained pressure, k is the creep rate constant, determining how quickly the deformation progresses over time, and a larger k value corresponds to a faster response.

The ESP32 NodeMCU-32S microcontroller reads analog voltages through a 12-bit ADC, mapping the voltage range of 0–5 V to digital values from 0 to 4095. As a result, all sensor outputs used in the analysis were digital readings in this range. To convert these sensor values into meaningful physical quantities, a cubic polynomial curve was fitted using calibration weights ranging from 200 to 1000 g. In this process, the x-axis represented the known weight applied to the sensor, and the y-axis represented the corresponding digital reading from the ESP32. Figure 2 shows the fitted curves obtained from the nine FSR406 sensors. Once the estimated weight was derived from the fitted function, it was normalized by dividing it by the maximum measurable weight corresponding to 5 V input. The result was a pressure percentage (0 to 1) that enabled consistent comparison across sensors.

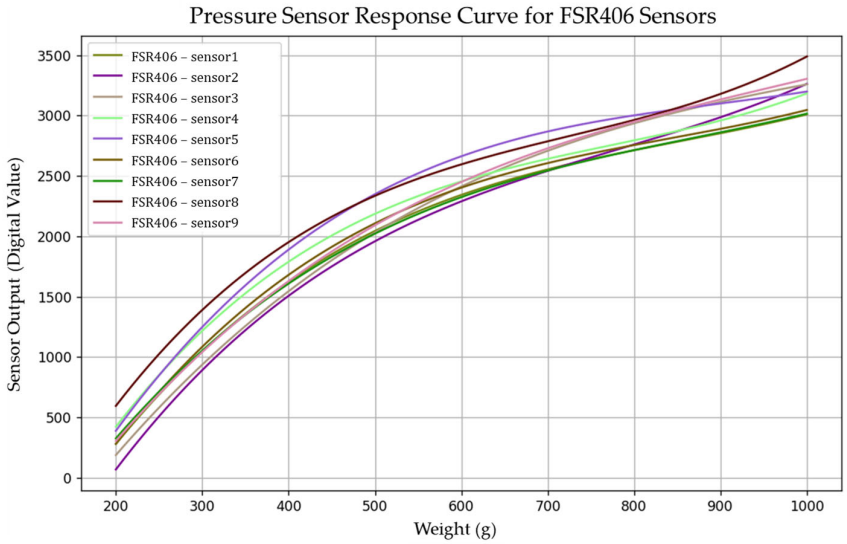


Figure 2. Pressure response curves of nine FSR406 sensors.

The final nine normalized values measured from the nine sensors were reshaped into a 3 × 3 matrix based on sensor layout and visualized as a heatmap. Figure 3 shows an example of the heatmap corresponding to the upright sitting posture.

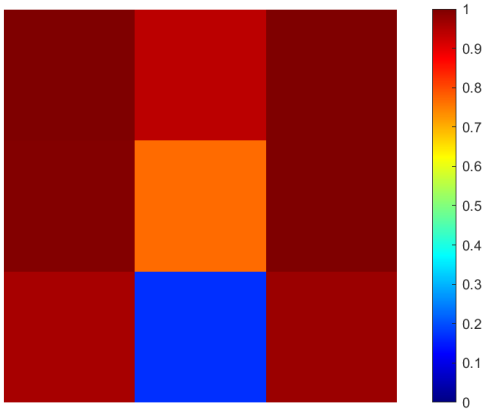


Figure 3. Posture pressure distribution heatmap. The map illustrates the pressure distribution across the sensor grid in a seated posture, where warmer colors indicate higher pressure and cooler colors indicate lower pressure.

2.3. Data Collection

10 healthy adult participants (5 males and 5 females) were recruited for this study. The participants' height ranged from 154 to 180 cm, and their body weight ranged from 52 to 96 kg. Each participant was instructed to perform nine predefined sitting postures. Each posture was maintained for 5 s and repeated three times. In total, 10 participants × 9 postures × 3 repetitions = 270 samples per participant, resulting in 1350 data samples across all participants.

2.4. Machine Learning Classification

Five supervised machine learning algorithms, decision tree, support vector machine (SVM), k-nearest neighbors (KNN), logistic regression, and narrow neural network, were implemented using MATLAB's Classification Learner, version R2025a. All models were trained with default parameters and no manual tuning. The input features included normalized pressure values from nine sensors and the participant's body mass index (BMI). Model performance was evaluated using classification accuracy as the primary metric. The classification accuracy is defined as the ratio of correctly predicted samples to the total number of samples:

$$\text{Accuracy} = \frac{TP + TN}{TP + TN + FP + FN} \tag{2}$$

where TP is true positive, TN is true negative, FP is false positive, and FN is false negative. Accuracy reflects the overall correctness of the model in predicting all posture classes.

3. Results

3.1. Posture Distribution Visualization

The normalized pressure data from nine sensors were reshaped into a 3 × 3 matrix based on sensor layout. For each posture, the corresponding matrix was converted into a heatmap for visual inspection as shown in Figure 4, showing distinct pressure patterns among different postures and demonstrating the effectiveness of the system in capturing posture-specific pressure distribution.

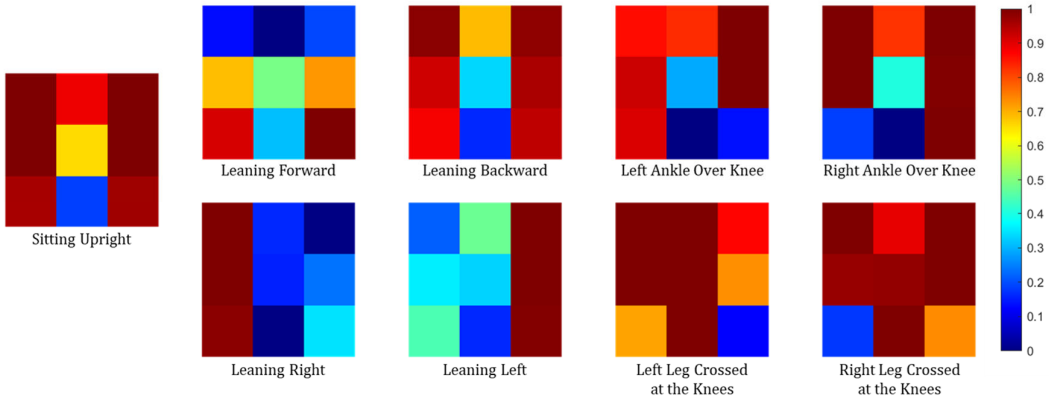


Figure 4. Pressure heatmaps for all nine sitting postures measured from the same subject: upright, leaning forward, leaning backward, leaning left, leaning right, as well as legs crossed at the knees and ankle over knee on both the left and right sides.

3.2. Model Performance Comparison

Five machine learning models were evaluated using classification accuracy. Table 1 summarizes validation and test accuracies before and after adding BMI as an additional feature. Without BMI, the narrow neural network achieved the best performance (91.73% test accuracy), followed by KNN and SVM. Decision tree and logistic regression performed slightly lower. After including BMI as the tenth input feature, test accuracy improved across most models. The narrow neural network and KNN maintained high performance, while logistic regression and SVM showed moderate gains. These results indicated that personal characteristics such as BMI improved posture classification by capturing individual differences in pressure distribution.

Table 1. Classification accuracy (%) of each model before and after adding BMI.

Model	Without BMI		With BMI	
	Accuracy % (Validation)	**Accuracy % (Test)**	**Accuracy % (Validation)**	**Accuracy % (Test)**
Tree	95.85	78.95	96	78.95
Efficient logistic regression	92.15	87.59	94.96	90.98
SVM	99.70	87.22	99.7	89.85
KNN	99.78	87.97	100	86.47
Narrow neural network	97.63	91.73	98.07	95.49

4. Discussion

The results demonstrated that the proposed system effectively distinguished different sitting postures based on pressure distribution. Among the five machine learning models tested, the narrow neural network achieved the highest classification accuracy, indicating its capability to capture nonlinear patterns in sensor data. SVM and KNN also performed well, while decision tree and logistic regression showed relatively lower accuracy, likely due to their simpler decision boundaries.

The inclusion of BMI as an additional input feature improved classification accuracy across all models. This suggested that body composition influences how pressure is distributed while sitting, and integrating personal features enhances model generalization. The improvement was most notable in models that initially had lower performance, such as logistic regression, highlighting the benefit of feature augmentation for simpler algorithms. The testing data were not randomly selected from the entire dataset. Instead, two out of ten participants were used exclusively for testing, while the remaining eight were used for

model training. This subject-independent validation setup resulted in lower test accuracy due to limited training diversity. However, adding BMI as a feature helped mitigate this issue by providing additional individual-level context for the models.

Overall, the use of pressure sensors combined with machine learning offers a non-intrusive method for posture classification. It is required to explore real-time posture recognition, timely user feedback, and long-term tracking of sitting behavior to enhance the system's practicality in daily environments.

5. Conclusions

We developed a smart cushion system that integrates pressure sensors and machine learning to classify sitting postures. The system effectively visualized pressure patterns using 3×3 heatmaps and achieved high classification accuracy across five models. The narrow neural network performed the best, and the addition of BMI as a feature further improved accuracy in all models. The results of this study highlighted the effectiveness of combining sensor-based input with personal features for posture classification. The system enables a non-intrusive and low-cost solution for daily sitting posture monitoring. Real-time implementation, personalized feedback, and long-term behavior tracking are required to enhance usability and practical value.

Author Contributions: Conceptualization, M.-C.L. and C.-F.J.; methodology, software, formal analysis, investigation, data curation, writing—original draft preparation, and visualization, M.-C.L.; resources, writing—review and editing, supervision, and project administration, C.-F.J. All authors have read and agreed to the published version of the manuscript.

Funding: This research received no external funding.

Institutional Review Board Statement: Not applicable.

Informed Consent Statement: Not applicable.

Data Availability Statement: The data that support the findings of this study are available from the corresponding author upon reasonable request.

Conflicts of Interest: The authors declare no conflict of interest.

References

1. Hamilton, M.T.; Hamilton, D.G.; Zderic, T.W. Role of Low Energy Expenditure and Sitting in Obesity, Metabolic Syndrome, Type 2 Diabetes, and Cardiovascular Disease. *Diabetes* **2007**, *56*, 2655–2667. [CrossRef] [PubMed]
2. Oakman, J.; Kinsman, N.; Stuckey, R.; Graham, M.; Weale, V. A Rapid Review of Mental and Physical Health Effects of Working at Home: How Do We Optimise Health? *Scand. J. Work Environ. Health* **2020**, *46*, 429–440. [CrossRef] [PubMed]
3. Koohsari, M.J.; Nakaya, T.; Shibata, A.; Ishii, K.; Liao, Y.; Oka, K. Working from Home After the COVID-19 Pandemic: The Role of Job Crafting, Work Engagement, and Self-Care Behavior. *Int. J. Environ. Res. Public Health* **2022**, *19*, 12344.
4. Tremblay, M.S.; Colley, R.C.; Saunders, T.J.; Healy, G.N.; Owen, N. Physiological and Health Implications of a Sedentary Lifestyle. *Appl. Physiol. Nutr. Metab.* **2010**, *35*, 725–740. [CrossRef] [PubMed]
5. Katzmarzyk, P.T.; Church, T.S.; Craig, C.L.; Bouchard, C. Sitting Time and Mortality from All Causes, Cardiovascular Disease, and Cancer. *Med. Sci. Sports Exerc.* **2009**, *41*, 998–1005. [CrossRef] [PubMed]
6. Szczygieł, E.; Zielonka, K.; Mętel, S.; Golec, J. Musculo-skeletal and pulmonary effects of sitting position—A systematic review. *Ann. Agric. Environ. Med.* **2017**, *24*, 8–12. [CrossRef] [PubMed]
7. Barsawade, V.; Dangare, S.; Jagadale, R.; Magdum, S.A. Study on incorrect sitting & standing posture and its implication on neck pain. *Int. Res. J. Eng. Technol.* **2019**, *6*, 1578.
8. O'Sullivan, K.; O'Keeffe, M.; O'Sullivan, L.; O'Sullivan, P.; Dankaerts, W. Perceptions of sitting posture among members of the community, both with and without non-specific chronic low back pain. *Man. Ther.* **2013**, *18*, 551–556. [CrossRef] [PubMed]
9. Jung, K.S.; Jung, J.H.; In, T.S.; Cho, H.Y. Effects of prolonged sitting with slumped posture on trunk muscular fatigue in adolescents with and without chronic lower back pain. *Medicina* **2020**, *57*, 3. [CrossRef] [PubMed]

10. Ma, S.; Cho, W.; Quan, C.; Lee, S. A Sitting Posture Recognition System Based on 3-Axis Accelerometer. In Proceedings of the 2016 IEEE Conference on Computational Intelligence in Bioinformatics and Computational Biology (CIBCB), Chiang Mai, Thailand, 5–7 October 2016; pp. 1–3.
11. Estrada, J.; Vea, L. Real-Time Human Sitting Posture Detection Using Mobile Devices. In Proceedings of the 2016 IEEE Region 10 Symposium (TENSYMP), Bali, Indonesia, 9–11 May 2016; pp. 140–144.
12. Estrada, J.; Vea, L. Sitting Posture Recognition for Computer Users Using Smartphones and a Web Camera. In Proceedings of the TENCON 2017—2017 IEEE Region 10 Conference, Penang, Malaysia, 5–8 November 2017; pp. 1520–1525.
13. Zhao, S.; Su, Y. Sitting Posture Recognition Based on the Computer's Camera. In Proceedings of the 2024 2nd Asia Conference on Computer Vision, Image Processing and Pattern Recognition, Xiamen, China, 26–28 January 2024.
14. Vagale, G.; Prajwal, G.K.; Kumar, R.; Dharishini, P.P.P. Computer Vision Assisted Deep Learning Based Sitting Posture Suggestion System. In Proceedings of the 2024 3rd International Conference on Intelligent Computing and Control Systems (ICICCS), Madurai, India, 15–17 May 2024; pp. 1–6.
15. Ahmad, J.; Andersson, H.; Sidén, J. Sitting Posture Recognition Using Screen Printed Large Area Pressure Sensors. In Proceedings of the 2017 IEEE Sensors, Glasgow, UK, 29 October–1 November 2017; pp. 1–3.
16. Suzuki, S.; Kudo, M.; Nakamura, A. Sitting Posture Diagnosis Using a Pressure Sensor Mat. In Proceedings of the 2016 IEEE International Conference on Identity, Security and Behavior Analysis (ISBA), Sendai, Japan, 29 February–2 March 2016; pp. 1–6.
17. Tsai, M.-C.; Chu, E.T.-H.; Lee, C.-R. An Automated Sitting Posture Recognition System Utilizing Pressure Sensors. *Sensors* **2023**, *23*, 5894. [CrossRef] [PubMed]
18. Lin, X.; Seet, B.C. A Linear Wide-Range Textile Pressure Sensor Integrally Embedded in Regular Fabric. *IEEE Sens. J.* **2015**, *15*, 5384–5385. [CrossRef]
19. Mallat, S.; Rochcongar, G. Calibration of Force Sensing Resistors (FSR) for Static and Dynamic Applications. In Proceedings of the IEEE International Conference on Robotics and Biomimetics, Tianjin, China, 14–18 December 2010; pp. 562–567.

Disclaimer/Publisher's Note: The statements, opinions and data contained in all publications are solely those of the individual author(s) and contributor(s) and not of MDPI and/or the editor(s). MDPI and/or the editor(s) disclaim responsibility for any injury to people or property resulting from any ideas, methods, instructions or products referred to in the content.